REPRODUCTION
RESEARCH

How, where and when is SPINK3 bound and removed from mouse sperm?

Anabella R Nicolli[1], Carlos A I Alonso[3], Catalina Otamendi[1], Micaela Cerletti[1], Ansgar Poetsch[4,6,7], Vikram Sharma[5], Lucia Zalazar[1], Silvina Perez-Martinez[2] and Andreina Cesari[1]

[1]Instituto de Investigaciones Biológicas (IIB-FCEyN/CONICET), Facultad de Ciencias Exactas y Naturales, Universidad Nacional de Mar del Plata, Consejo Nacional de Investigaciones Científicas y Técnicas (CONICET), Mar del Plata, Argentina, [2]Centro de Estudios Farmacológicos y Botánicos (CEFYBO-UBA/CONICET), Facultad de Medicina, Universidad de Buenos Aires, Consejo Nacional de Investigaciones Científicas Técnicas, Buenos Aires, Argentina, [3]Department of Pharmacology and Therapeutics, McGill University, Montréal, Canada, [4]Plant Biochemistry, Ruhr University Bochum, Bochum, Germany, [5]School of Biomedical Science, University of Plymouth, Plymouth, UK, [6]Queen Mary School, Medical College, Nanchang University, Nanchang, China and [7]College of Marine Life Sciences, Ocean University of China, Qingdao, China

Correspondence should be addressed to A R Nicolli; Email: anabellanicolli@gmail.com

Abstract

Sperm capacitation in mammals is a fundamental requirement to acquire their fertilizing capacity. Little is known about the action mechanism of the molecules that prevent capacitation from occurring prematurely. These molecules are known as decapacitation factors (DFs) and they must be removed from the sperm surface for capacitation to occur successfully. Serine protease inhibitor Kazal type 3 (SPINK3) has been proposed as one of these DFs. Here, we evaluate how this protein binds to mouse sperm and its removal kinetics. We describe that SPINK3 is capable of binding to the membrane of mature epididymal sperm through protein–lipid interactions, specifically to lipid rafts subcellular fraction. Moreover, cholera toxin subunit b (CTB) avoids SPINK3 binding. We observe that SPINK3 is removed from the sperm under *in vitro* capacitating conditions and by the uterine fluid from estrus females. Our *ex vivo* studies show the removal kinetics of this protein within the female tract, losing SPINK3 formerly from the apical region of the sperm in the uterus and later from the flagellar region within the oviduct. The presence of acrosome-reacted sperm in the female duct concurs with the absence of SPINK3 over its surface.

Reproduction (2022) **163** 251–266

Introduction

Capacitation in mammals is known as the biochemical and physiological modifications that sperm undergoes to acquire its fertilizing capacity (Chang 1951, Austin 1952). When capacitation begins, cholesterol is removed from the sperm plasma membrane, causing structural changes and allowing an increase in the permeability of the sperm to calcium (Ca^{2+}) and bicarbonate (Puga Molina *et al.* 2018). Intracellular increase of these ions activates adenyl cyclase leading to increased cAMP and the consequent activation of cAMP-dependent protein kinase and its downstream signaling pathways (Stival *et al.* 2015, Graf *et al.* 2020). In this process, the plasma membrane undergoes a reorganization of proteins and lipids (Cross 2004, Harrison & Gadella 2005). Ultimately, capacitation leads to two physiological processes: an acrosomal reaction (AR) and hyperactivation of the flagellum.

Decapacitation factors (DFs) have been studied since the 1950s (Chang 1957, Bedford & Chang 1962, Fraser 1984). The sperm surface is continually remodeled after spermiogenesis by molecules secreted from the epididymis and the secretory male glands composing the seminal plasma fluid (Leahy & Gadella 2011). DFs proteins modify the sperm physiology regulating the time and place of capacitation (Yanagimachi 1994, Nixon *et al.* 2006). In order to get a successful capacitation, the DFs must be removed.

Many proteolityc enzyme inhibitors have been reported in the epididymis and male accesory gland secretions. HongrES1, from the SERPIN family, has been reported in mouse as a regulator of sperm capacitation (Zhou *et al.* 2008). The Kazal-like family of serine protease inhibitors (SPINK) is found in abundance in the male germ cells as well as in the male genital fluids (Odet *et al.* 2006, Raterman & Springer 2008, Yamashita *et al.* 2008, Sipila *et al.* 2009, Cesari *et al.* 2010, Lu

ISSN 1470–1626 (paper) 1741–7899 (online)
https://doi.org/10.1530/REP-21-0195
Online version via https://rep.bioscientifica.com

et al. 2011, O'Rand *et al.* 2011, Kherraf *et al.* 2017, Shang *et al.* 2018). In mice, four epididymis-specific Spink genes – Spink8, Spink10, Spink11 and Spink12 – each with a distinctive regional expression pattern in the epididymis, have been identified (Jalkanen *et al.* 2006). Serine protease inhibitor Kazal-type-like (SPINKL) and serine protease inhibitor Kazal type 3 (SPINK3) are expressed in mouse seminal vesicles. SPINKL was reported to act as a decapacitation factor to prevent sperm from precocious capacitation (Lin *et al.* 2008, Tseng *et al.* 2013). Also, SPINK3, a small inhibitory protein of the Kazal type 3 serine protease, has been described as a potential decapacitation factor.

SPINK3 is secreted by the seminal vesicle into seminal fluid where it adheres to the surface of mouse sperm (Chen *et al.* 1998, Ou *et al.* 2012, Zalazar *et al.* 2012, Assis *et al.* 2013). Previous studies showed that SPINK3 expression is not detected in the epididymis (Chen *et al.* 1998). SPINK3 regulates capacitation by affecting Src activation and consequently the membrane hyperpolarization and the AR. In turn, it has been observed that Ca^{2+} entry into the cell is inhibited in the presence of this molecule, suggesting that it could be blocking the main calcium entry channel (CatSper) either directly or indirectly (Zalazar *et al.* 2020).

DFs attach to the apical portion of the head and/or to the flagellum of mouse spermatozoa (Nixon *et al.* 2006, Zalazar *et al.* 2020). However, there is no consensus on their binding mechanisms and the molecules involved therein. It has been proposed that DFs attachment is mediated by protein–membrane lipids interactions (Brewis & Gadella 2009). Many molecular interactions in the form of protein–protein interactions (PPIs) should also mediate the attachment of sperm-binding proteins; however, to date, due to the difficulties in analyzing *in vivo* membrane PPIs, there are insufficient reports for DFs. At the same time, the removal of DFs from the sperm surface in the female tract has been studied to a lesser extent.

Particularly for SPINK3, while the mechanism of action at the molecular level has been examined, little is known about its binding and removal kinetics and mechanisms. Previous studies by Ou *et al.* (2012) suggest that certain specific conditions of the female tract allow the release of the decapacitation factor in the uterus. The objective of this work is focused on evaluating how and where SPINK3 associates with and detaches from the sperm surface in the murine model. We evaluate the site, the kinetic and the release mechanism of SPINK3 from the sperm surface.

Materials and methods

Reagents: Unless otherwise stated, products were sourced from Sigma-Aldrich and were of the highest reagent grade available. Probes: Annexin V/FITC (Miltenyi Biotec, Bergisch Gladbach, Germany; 130093060), Cholera toxin subunit beta Alexa fluor 594 conjugate (Invitrogen, C34777), PNA Alexa fluor 594 (Molecular Probes, L32459); Primary Antibodies: anti-caveolin (BD Biosciences, 610060), anti-Gapdh (Sanllorenti *et al.* 1992), anti-flotillin (Abcam, ab41927), anti-SPINK3 (Sigma-Aldrich, HPA027498), anti-SPINK3 (Sigma-Aldrich, WH0006690M1). Secondary antibodies: anti-mouse IgG Alexa 488 (Abcam, ab15105), anti-rabbit IgG Alexa 555 (Abcam, ab150074), anti-rabbit IgG Alexa 488 (Thermo Fisher, A11070), and HRP-conjugated anti-rabbit (Sigma-Aldrich, A0545).

Animals

BALB/c mice (*Mus musculus*) were maintained at 22°C with a photoperiod of 12 h light:12 h darkness, food and water *ad libitum*. Sexually mature (2–3 months) male and female mice were euthanized by cervical dislocation. All procedures were approved by the local Institutional Animal Care and Welfare Committee from the National University of Mar del Plata (RD 225/16, RD 378/19), following the National Institutes of Health Guide to the Care and Use of Laboratory Animals.

Heterologous expression of recombinant SPINK3

In this study, we employed two different versions of recombinant SPINK3, SPINK3-His_6 and GST-SPINK3. The use of one or the other was based on the specific aim of each experiment.

For the production of SPINK3-His_6, the cDNA encoding the mature SPINK3 from *M. musculus* (NCBI ID: NM 009258.5) was cloned into the pET-24b(+) (Novagen, Madison, WI, USA) expression vector. Overexpression of SPINK3 was performed in *Escherichia coli* Rosetta cells (Novagen) and the recombinant protein was purified to apparent homogeneity by a HiTrap IMAC HP (GE Healthcare Life Sciences) affinity chromatography as described in a previous work (Assis *et al.* 2013). Purified recombinant protein was dialyzed against phosphate-buffered saline (PBS, 10 mM phosphate buffer, 137 mM NaCl and 2.7 mM KCl pH 7.4). The antibody α-SPINK1 recognized SPINK3 with an efficiency over than 82% (Zalazar *et al.* 2012); this is because the homologous gene designated for SPINK3 is actually SPINK1, which was originally isolated from the pancreas as an inhibitor of trypsin and other serine proteases (Kazal *et al.* 1948, Turpeinen *et al.* 1988).

For the immobilization of GST-SPINK3 on sepharose beads, the cDNA encoding SPINK3 was cloned into a pGEX-4T-3 expression vector (GE) downstream of the GST coding sequence, expressed, purified and crosslinked to Glutathione Sepharose 4B as described previously (Zalazar *et al.* 2014).

Sperm preparation

Epididymides were dissected in *cauda*, *corpus* or *caput* regions. When indicated, respective regions for each assay were immersed in PBS, HM medium (Modified Krebs Ringer Bicarbonate medium: 20 mM Hepes, 119.3 mM NaCl, 4.7 mM KCl, 1.2 mM $MgSO_4$, 5.6 mM glucose, 1.2 mM KH_2PO_4, 0.5 mM Na pyruvate and 1.7 mM $CaCl_2$; pH 7.4) or Annexin V binding buffer (10 mM Hepes, 5 mM KCl, 1 mM $MgCl_2$, 150 mM NaCl, 1.8 mM $CaCl_2$; pH 7.2) in culture dishes on a warm plate at 37°C. The tissues were minced with scissors to allow

the sperm dispersion into the media. After 10 min, once the sperm was dispersed in the media, the tissue was pulled out and non-capacitated sperm was washed with fresh PBS, HM medium or Annexin V binding buffer by mild centrifugation for 10 min at 800 ×***g***.

Sperm capacitation

For capacitation conditions, 25 mM $NaHCO_3$ and 3 mg mL^{-1} BSA (HMB) were added to sperm in HM. Then, sperm were incubated in an atmosphere of 5% CO_2 at 37°C for at least 60 min (7.5×10^6 cells mL^{-1}). When capacitation was performed in the presence of SPINK3 (13 µM) (Samanta *et al.* 2018, Noda & Ikawa 2019), sperm were pre-incubated for 15 min at 37°C with recombinant protein SPINK3-His_6 at the beginning of the assay (Zalazar *et al.* 2020).

When indicated, capacitation was initiated by methyl-β-cyclodextrin (MβCD) (0.8 mM) for 15 min at room temperature.

Protein extracts and subcellular fractionation

Solubilized membrane proteins and membrane rafts were prepared following the standard laboratory protocols. Briefly, caudal epididymal sperm were washed and resuspended in 2.5 mL of TEN buffer (10 mM Tris-HCl, 1 mM EDTA, 10 mM NaCl, pH 7.5). Sperm concentration was calculated using a Neubauer chamber. The cells were subjected to cold sonication for five pulses of 30 s at a power of 60 Hz, with intervals of 30 s, followed by 1 h incubation at 4°C in the presence of 0.5% (v/v) of Triton X-100. Then, the solution was centrifuged for 20 min at 12,000 ×***g*** at 4°C, recovering both the soluble and insoluble fraction of the preparation.

The precipitate was resuspended in TEN buffer and stored at −20°C as the membrane fraction until use. The volume of the supernatant was measured and an equal volume of 80% (w/v) sucrose in TEN buffer was added in order to achieve a concentration of 40% (w/v). An isopycnic sucrose gradient was composed from bottom to top by 750 µL layers of the protein fraction in 40% sucrose, followed by 30 and 5% sucrose layers. The total sample was divided into eight columns that were centrifuged at 70,000 ×***g*** at 4°C for 18 hs. Then, 200 µL fractions were collected from the top to the bottom of each column (fractions 1–9). Pooled fractions were dialyzed against PBS and concentrated four times using 3 kDa ultrafiltration membranes (Amicon). The raft fraction was confirmed by western blot using a specific anti-caveolin antibody (1: 1000, BD Biosciences, 610060). To obtain the cytosolic fraction, cauda epididymal sperm were collected from three mice, as it was described previously. The cells were sonicated and resuspended in TEN buffer and centrifuged for 120 min at 200,000 ×***g***. The supernatant was resuspended and centrifuged again for 120 min at 200,000 ×***g***, separating the cytosol fraction. Each fraction was analyzed by western blot using an anti-GAPDH antibody (1: 25000, Sanllorenti *et al.* 1992) and anti-caveolin (1: 1000, BD Biosciences, 610060) in order to analyze their content (data not shown).

Pancreatic protein extracts were prepared as follows. Briefly, pancreas from mice were resuspended in TEN buffer (1.5 µL buffer per milligram of tissue). Homogenates were obtained by using a homogenizer (IKAWERKE T10 basic Ultra- Turrax®, S10N-8G dispersing tip) for two pulses of 60 s, with intervals of 2 min. Homogenates were centrifuged for 25 min at 20,000 ×***g*** at 4°C, recovering the soluble fraction of the preparation and ultra-centrifugated for 40 min at 76,000 ***g*** at 4°C. The supernatant was stored at −80°C until use.

Uterine fluid preparation

For uterine fluid (UF) preparation, different stages of the estrus cycle were determined by observation of vaginal epithelium cells (Byers *et al.* 2012). This was performed over BALB/c strain (2–6 months) female mice. For UF preparation, sexually mature female mice of the BALB/c strain (2–6 months), different stages of the estrus cycle were determined at the observation of cells of the vaginal epithelium (Byers *et al.* 2012). Females were euthanized by cervical dislocation. The uterus was extracted and flushed with PBS; the fluid obtained was centrifuged at 11,180 ×***g*** for 10 min at 4°C to remove cellular debris. The supernatant was stored at −80°C until used. Physiological status of the fluid was verified by microscopic observation of motile cilia of oviduct ciliated epithelial cells before centrifugation accounting for viability of the sample.

Protein concentration was determined by a Nano-Drop instrument.

Preparation of total sperm membrane lipids

Total membrane lipids of sperm were obtained using a variant of the technique described in Bligh and Dyer (1959). A total of 7×10^5 cells were mixed with a chloroform: methanol (2:1) solution. The samples were centrifuged at 2500 ×***g*** for 10 min to carry out phase separation. The organic phase was recuperated, and it was evaporated using a Savant AES 1010 SpeedVac Concentrator. The pellet was stored at −20°C until used and resuspended in 20 µL of chloroform for blotting.

Annexin V labeling

In order to assess phosphatidylserine-type phospholipid exposure in spermatozoa, epididymides from mature mice were immersed in Annexin V binding buffer, washed and set to a concentration of 5×10^6 cells mL^{-1}. Sperm (100 µL) were incubated with 10 µL solution Annexin V-FITC conjugated (Miltenybiotec, 5150324353) for 15 min at room temperature in the dark. Cells were washed in Annexin V binding buffer for 5 min at 800 ×***g***, after washing, cells were placed on slides and fluorescence was observed under a 480/525 nm filter on a microscope: Nikon Eclipse T2000 at 1000× magnification.

Dot-blot assay

For the assessment of the interaction assays between SPINK3 and subcellular fractions, protein-containing fractions membrane, rafts, cytosolic proteins or recombinant SPINK3-His_6 (3 µg) spot seeded on nitrocellulose membranes (0.06 µg) and incubated in the presence or absence of SPINK3-His_6 (13 µM) for 120 min at 4°C in PBS. Subsequently, membranes were washed to eliminate non bound protein and blocked for

45 min with 1% BSA (w/v) in PBS. Then, they were incubated with the following primary antibodies: anti-SPINK3 (1:500, Sigma-Aldrich, HPA027498), anti-caveolin (1:1000, BD Biosciences, 610060) or anti-Gapdh (1:25,000, Sanllorenti *et al.* 1992). The immunoreactions were developed with HRP-conjugated anti-rabbit (1:10,000, Sigma-Aldrich, A0545) and visualized with a C-Digit chemiluminescence reader (Li-Cor).

For the assays of interaction between SPINK3-His_6 lipids, total membrane extract or different amounts (as indicated) of phosphatidylcholine (PC, Avanti Polar Lipids, Alabaster, AL, USA; 840051), phosphatidylserine (PS, Avanti Polar Lipids, 840032) and cholesterol (Cho, Sigma-Aldrich, C8667) dissolved in chloroform, and the monosialotetrahexosylganglioside GM1 (GM1, Cayman Chemical, 19579) dissolved in DMSO, were spot seeded on nitrocellulose membranes. The membranes were blocked for 60 min with 3% BSA in PBS. Then, they were incubated in the presence or absence of 13 µM SPINK3-His_6 overnight. After washing and blocking (3% BSA 0.1% Tween 20 in PBS) for 45 min, interaction was assessed with anti-SPINK3 as described above. As a positive control 3 µg of SPINK3 was dotted, as indicated.

Competition and removal assays

To evaluate the remotion of SPINK3-His_6 by *in vitro* capacitation, sperm were incubated in HMB as indicated (section: Sperm preparation) and aliquots were evaluated by immunofluorescence at the following times: 0, 15, 30, 60 and 90 min. To evaluate the ability of UF to remove SPINK3-His_6 from the sperm surface, cells (1×10^7 cells mL^{-1} in 100 µL PBS) were incubated with UF from estrus or metaestrus females (24 µg protein; based on the average protein concentration obtained in the extraction of UF). Aliquots were taken at 15 and 30 min, washed and the presence of SPINK3-His_6 was detected by immunofluorescence (see below).

A competition assay between SPINK3 and cholera toxin was carried out for GM1-rich regions. GM1 was located by a specific probe cholera toxin subunit beta Alexa Fluor 594 conjugate (CTB, Invitrogen, C34777). Two competition conditions were set up: (i) Sperm from cauda epididymis were obtained in PBS as previously described and were incubated with or without 4 mM CTB at 37°C for 60 min (1×10^7 cells mL^{-1}) and further incubated in the presence or absence of SPINK3-His_6 13 µM for 15 min at 37°C; (ii) Sperm were incubated with SPINK3 13 µM for 15 min at 37°C and 4 mM CTB was added for 60 min. Cells were fixed for 30 min at room temperature with 4% paraformaldehyde and washed (800 ***g*** 15 min), laid on the slides, dried, fixed with 96% ethanol and washed in PBS. Immunofluorescence assay was performed to detect SPINK3 as described in the following section. The CTB probe was visualized in the red channel.

In vitro immunodetection of SPINK3-His_6 and flotillin on the sperm surface

For immunodetection, spermatozoa were obtained as previously described and incubated in presence or absence of 13 µM SPINK3-His_6 for 15 min at 37°C under non-capacitating conditions to allow binding and washed for 10 min at 800 ×***g*** to remove non-bound protein.

Immunofluorescence was carried out as follows: Cells were fixed in 0.4% (v/v) formaldehyde, washed and dried on slides. After washing and blocking (3% BSA (w/v)), the slides were incubated either with rabbit anti-SPINK3 (1:50, Sigma-Aldrich, HPA027498), mouse anti-SPINK3 (1:50, Sigma-Aldrich, WH0006690M1) or rabbit anti-flotilin (1:50, Abcam, ab41927), as indicated. Secondary antibodies anti-mouse IgG-Alexa 488 (1:500, Abcam, ab15105), anti-rabbit IgG-Alexa 555 (1:500, Abcam, ab150074) or anti-rabbit IgG-Alexa 488 (1:1000, Thermo Fisher, A11070) were used when indicated. The mounting was carried out with DABCO (Sigma-Aldrich 290734) and the cells were observed under a confocal microscope (Olympus FV1000) in a co-immunodetection assay. For assays that evaluate SPINK3-His_6 detachment, the slides were mounted with glycerol: PBS (9:1) and fluorescence was observed under a 480/525 nm filter on a microscope: Nikon Eclipse T2000 at 400× or 1000× magnification.

The rabbit anti-SPINK3 specificity was evaluated in samples without SPINK3-His_6 and the control of the secondary antibody was carried out by incubating without the respective primary antibodies (data not shown).

Ex vivo immunolocalization of SPINK3 and acrosomal status

For each assay, four sexually mature females were placed in a cage with male bedding for 68 h before coitus to synchronize estrus. On the day of the experiment, three female mice were placed in a cage with a sexually mature male at lights off. The animals were monitored all along the experimental time until copulation behavior was detected. The time when the copulation plug was first found was recorded as 0 h *post coitus*. At this time, the female mice were removed from the cages. Females were euthanized at 0, 1.5 and 3 h *post coitus* by cervical dislocation and the entire uterus and oviduct were dissected. On the first euthanized female (0 h *post coitus*) flushing of the uterine horns was performed with PBS medium, fluid was collected, and cells were pelleted (800 ×***g*** for 8 min),d the sperm concentration adjusted to 1×10^7 cells mL^{-1}, placed onto glass slides and fixed/permeabilized with 96% ethanol. At 1.5 and 3 h *post coitus*, the female tract was dissected and cryocuts of the different regions (uterus–uterine–tubal junction–isthmus) were carried out, mounted and fixed for 10 min in 100% acetone.

Cells and histological cuts were blocked (3% BSA in PBS), incubated with rabbit anti-SPINK3 (1:50, Sigma-Aldrich, HPA027498) and developed with anti-rabbit IgG-Alexa 488 (1:1000, Abcam, ab15105). For acrosome status assessment, PNA Alexa fluor 594 (1µL mL^{-1}, Molecular Probes, L-32459) was added simultaneously with the secondary antibody, when indicated. Slides were washed and mounted with glycerol: PBS (9:1) and fluorescence was observed under 480/525 nm filter on the microscope at 400× or 1000× magnification. The specificity of the antibody was assessed in samples without SPINK3, and secondary antibody control was performed by incubation without the respective primary antibodies.

Protein–protein interaction assays

Samples of UF from females in estrus, sperm membrane extract or pancreatic protein extracts (containing positive control trypsin) (30 µg of total protein) were charged on matrix with GST-SPINK3, or GST immobilized in glutathione-agarose 4D (1 mL, GE Life Science, 17-0756-01) and kept for 60 min at room temperature under stirring as described previously (Zalazar *et al.* 2014). Briefly, the immobilization of the protein was performed by the bifunctional cross-linker dithiobis (succinimidyl propionate) and the reliability of the cross-linking procedure was confirmed by analyzing the leakage produced by the elution buffer. The retained proteins were purified according to the previously described protocol (Zalazar *et al.* 2014). Briefly, the column was washed with 10 volumes of PBS and the retained proteins were eluted with five volumes of 8 mM glutathione reduced in 50 mM Tris–HCl, pH 8.

The purified complexes were visualized by SDS-PAGE on 12% (w/v) acrylamide gels, with Coomassie Brilliant Blue (Laemmli *et al.* 1970). The gel was divided into two sections (UP and DOWN), cut into small cubes and destained as described in Cerletti *et al.* (2018*a*). Gel pieces were dried using a SpeedVac and incubated with trypsin (porcine, sequencing grade, Promega) solution (12.5 ng mL^{-1} in 25 mM ammonium bicarbonate, pH 8.6) overnight at 37°C with agitation (tempered shaker HLC MHR20, 550 rpm). After digestion, the peptides were eluted by adding elution buffer (50% acetonitrile, 0.5% TFA, UPLC grade, Biosolve, the Netherlands) (1 µL elution buffer for each microliter of digestion buffer) and sonicated for 20 min in an ultrasonic bath. The samples were centrifuged and the supernatants were transferred to new 1.5 mL tubes. The extracted peptides were dried using a SpeedVac and stored at −20°C. Before Mass spectrometry (MS) analysis, peptides were re-suspended in 20 µL of buffer A (0.1% formic acid in water, ULC/MS, Biosolve, the Netherlands) by sonication for 10 min and transferred to liquid chromatography–mass spectrometry grade glass vials (12 × 32 mm glass screw neck vial, Waters, Milford, MA, USA). Each measurement was performed with 8 µL of the sample. Protein samples were subjected to LC-ESI-MS/MS using a nano ACQUITY gradient UPLC pump system (Waters) and an LTQ Orbitrap Elite mass spectrometer as described in Cerletti *et al.* (2018*a*).

Proteins were identified and quantified with MaxQuant version 1.5.3.17 using the LFQ algorithm searching against the Uniprot *M. musculus* database (downloaded in October 2021). The parameters were set as described in Cerletti et al. (2018*b*): main search peptide mass tolerance of 4.5 ppm, minimum peptide length of six amino acids with maximum two missed cleavages, routine post-translational modifications were searched including variable oxidation of methionine, deamidation (NQ), N-terminal glu→pyroglutamate, and protein N-terminal acetylation, LFQminimum ratio count of 2, matching between runs enabled, PSM and (Razor) protein FDR of 0.01, advanced ratio estimation and second peptides enabled. FDR was set to 0.05 using the permutation of data between samples implemented in Perseus (Tyanova *et al.* 2016) (250 permutations, S0 = 0.1). Proteins were considered to be potential SPINK3 interactors if they were detected only in the SPINK3 condition in at least two replicates and they contained secretory motives.

Determination of trypsin activity by zymography

Proteolytic activity was assessed in 12% (w/v) polyacrylamide gels copolymerized with 1% gelatin (Manchenko 2002). SDS-PAGE was run at 4°C and 15 mA under non-denaturing conditions. SDS was eliminated by 2.5% Triton X-100 followed by incubation in 10 mM $CaCl_2$ and finally with distilled water. Gels were incubated at 50 mM Tris–HCl, pH 7.5 overnight at 37°C. The result was revealed with Coomassie Brilliant Blue R-250 (Hummel *et al.* 1996). The proteolytic activity was determined through the visualization of clear bands (degraded gelatin) in a dark background.

Statistical analysis

Data from experiments were analyzed by GLMM (generalized linear mixed effect model) to determine statistical significance between treatments and control (Zuur *et al.* 2009). The model included the male variable as a random effect. Normality of residuals was assessed by plotting theoretical quantiles vs standardized residuals (Q–Q plots). Homogeneity of variance was evaluated by plotting residuals vs fitted values. A *post hoc* analysis was conducted with the 'lsmeans'' package (Lenth 2016). All analyzes were performed using R software version 3.3.33, with the 'nlme' package for Gaussian models (Pinheiro *et al.* 2007). For all analyzes, statistically significant differences were determined at $P < 0.05$. Graph bars indicate mean ± S.E.

Results

Binding of SPINK3 to the plasma membrane of mouse sperm

Given the membrane remodeling that occurs to sperm during epididymal transit, we were interested in evaluating whether these changes render sperm the ability to bind SPINK3. Thus, we incubated recombinant SPINK3 with sperm from different sections of the epididymis. Results showed that sperm from cauda presented an immunospecific signal of SPINK3 (Fig. 1), suggesting that only the membrane from mature sperm has a SPINK3 acceptor. The immunospecific signal of SPINK3 was observed both over the apical region and the principal piece of the cauda spermatozoa.

In order to evaluate whether SPINK3 is able to bind sperm proteins, mature sperm extracts were confronted to immobilized GST-SPINK3 in a glutathione agarose column and the retained fraction was analyzed by SDS-PAGE (Fig. 2A and B). While in control pancreas (PAN) extract a protein band compatible with the known SPINK3 interactor trypsin was detected (Fig. 2B, lanes 4 and 5), no protein was attached to the column in the sperm (SPZ) samples (Fig. 2B, lane 2), suggesting that either there is no protein tag for this DFs in sperm or that this union is not stable enough under the assayed conditions.

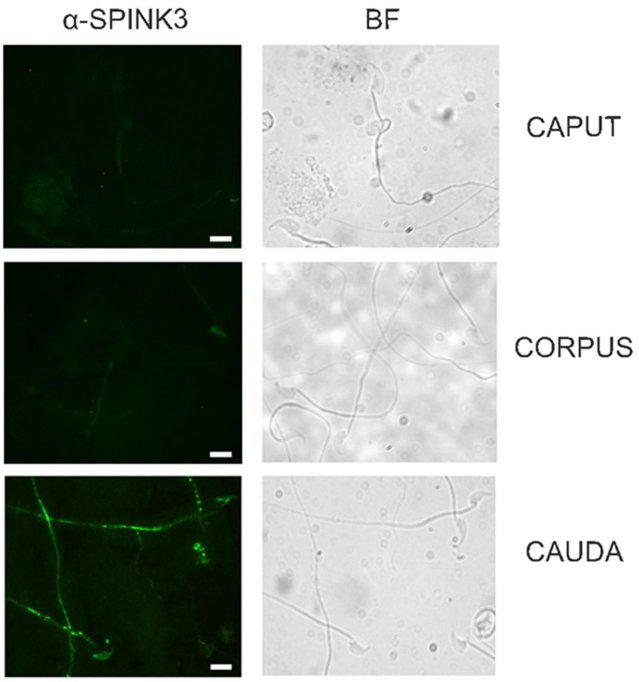

Figure 1 SPINK3-His_6 binds to mature sperm. Immunodetection of recombinant SPINK3 binding to sperm from different epididymal sections. Mouse epididymis sperm from cauda, corpus or caput sperm were incubated in the presence of SPINK3-His_6 (13 μM) and immunofluorescence assays were performed using rabbit anti-SPINK3 (α-SPINK3) followed by anti-rabbit IgG-Alexa488 (green). Scale bar: 10 μm. The images are representative images from three independent experiments. BF, bright field.

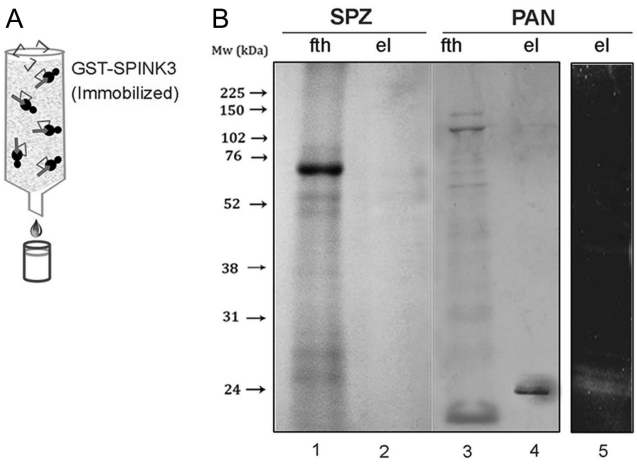

Figure 2 Interaction of sperm protein extracts with GST-SPINK3 baited Glutathione Sepharose column. (A) Schematic representation of the method for purification of ligands with binding affinity to a GST-SPINK3. GST or GST-SPINK3 were immobilized to glutathione (GSH)–agarose affinity column (Zalazar *et al.* 2014). (GST portion symbolized as a circle + bait protein symbolized as a '→', mobile phase symbolized as ∏). (B) Electrophoretic separation of putative protein interactors. Sperm protein extracts (SPZ, 74 × 10^6 cells, 1 mg) or pancreas protein extracts (PAN, 1 mg), were loaded onto the column. Flowthrough (fth) and non-retained proteins were collected by washing and retained proteins were eluted by 0.2 M glycine–HCl pH 2.6 and neutralized by 2 M Tris–HCl, pH 9. Fth and eluted (el) proteins (5 μg) were separated by SDS-PAGE in 12% acrylamide gels. The proteolytic activity of the protein from pancreas with electrophoretic mobility corresponding to trypsin was determined by zymography (right panel). The images are representative of three independent experiments.

To test whether SPINK3 interacts with sperm through protein–lipid interactions, we incubated immobilized sperm lipid extracts with or without SPINK3. As shown in Fig. 3A, SPINK3 is able to interact with sperm membrane lipid extracts. To determine which lipids can interact with SPINK3, the assay was repeated with immobilized phosphatidylcholine (PC), phosphatidylserine (PS), cholesterol (Cho) and monosialotetrahexosylganglioside (GM1). SPINK3 interacted with the highest concentrations of PC, while the interaction with PS was dose dependent up to 0.1 μM (Fig. 3B). No interaction with cholesterol or GM1 was detected. PS exposure in non-capacitated sperm was evaluated by Annexin V labeling (Fig. 3C). A basal PS revelation was observed along the post acrosomal and midpiece regions.

To study if SPINK3 binds to specific regions of the plasma membrane such as lipid rafts, different membrane fractions were immobilized and exposed to SPINK3. Cellular fractions were validated by antibodies against marker proteins (Fig. 4A, lower panels). The fractions corresponding to the whole membrane (F9) and membrane rafts (F7) showed a greater binding affinity to SPINK3 (Fig. 4A, upper lane). Moreover, distribution of SPINK3 binding regions in the cells was similar to flotillin rich regions in the apical section of the head and principal piece (Fig. 4B). As these microdomains are stabilized by enriched cholesterol and sphingolipid regions (Kawano 2008) we studied if cholera toxin subunit B (CTB) competitively displaced SPINK3 binding to the sperm surface (Fig. 5). Sperm preincubated with CTB did not show SPINK3 immunolabeling while previous incubation with SPINK3 was not able to avoid CTB binding to most sperm, suggesting that pentameric CTB compete with SPINK3 for binding sites, but SPINK3 was not sufficient to block CTB-GM1 interaction.

SPINK3 is removed in the within a capacitating environment

It has been reported that SPINK3 was removed from the sperm head in the uterus of the female mice (Ou *et al.* 2012). However, we have recently reported that *in vivo* distribution of SPINK3 in non-capacitated sperm is also along the principal piece, where it might be regulating CatSper or Slo3 channels. Moreover, already capacitated sperm was no longer able to bind SPINK3 (Zalazar *et al.* 2020). To determine if *in vitro* capacitation *per se* could remove the recombinant SPINK3, immunodetection assays were carried out under both capacitating and non-capacitating conditions at different times. We

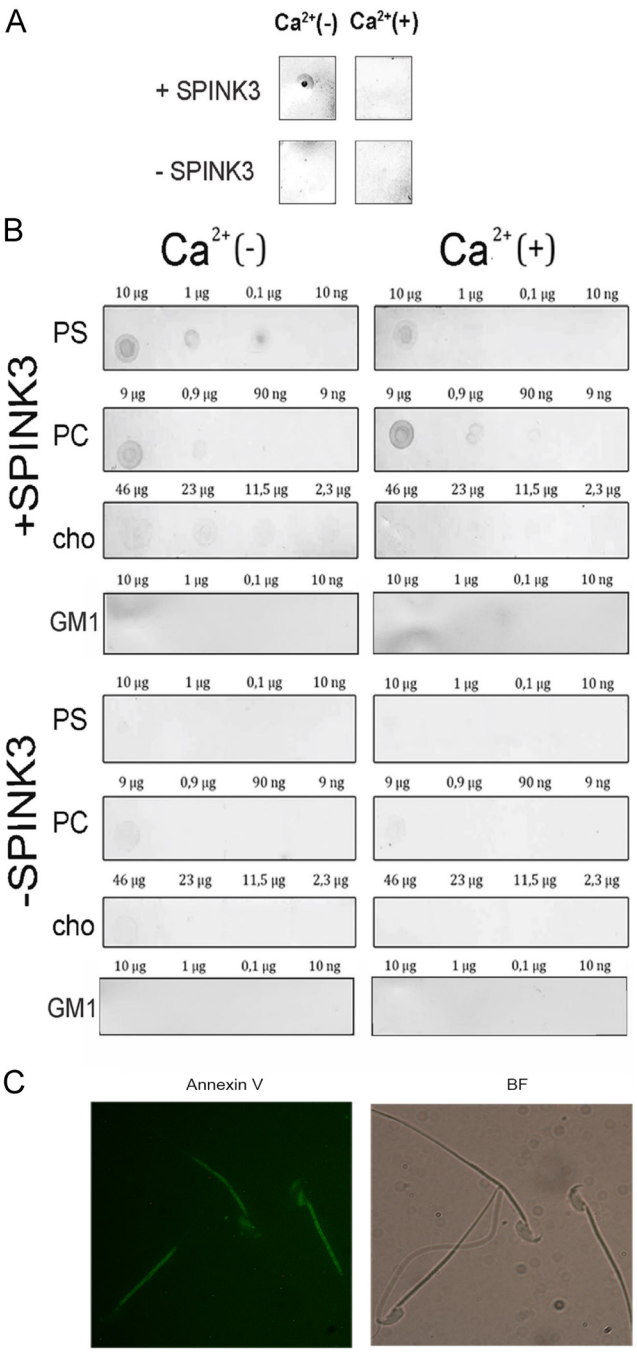

Figure 3 Interaction of SPINK3-His_6 with membrane lipids. (A) A membrane lipid extract obtained from 1×10^7 cells or (B) the indicated amounts of commercial PS, PC, Cho and GM1 were spot seeded on a nitrocellulose membrane that was then incubated SPINK3-His_6 (13 µM). The interaction was revealed by immunoblotting. (C) Annexin V staining of non-capacitated sperm showing basal exposure of PS. The images are representative of three independent experiments. Cho, cholesterol; GM1, monosialotetrahexosylganglioside GM1; PC, phosphatidylcholine; PS, phosphatidylserine.

observed that *in vitro* capacitation triggered by BSA and sodium bicarbonate decreased the percentage of cells showing SPINK3 bound to the surface compared to the non-capacitating condition (Fig. 6A, bottom panel $P < 0.05$). Detachment of SPINK3 from the principal piece was detectable at 15 min after incubation of the cells under capacitating conditions (Fig. 6A), suggesting that capacitation-mediated membrane changes are sufficient to promote the release of SPINK3 from the sperm surface. Note that it has been previously demonstrated that BSA is not capable of removing SPINK3 (Zalazar *et al.* 2020). As we previously showed that SPINK3 binds to raft regions of the sperm membrane, raft destabilization caused by capacitation was monitored by alterations in flotillin distribution. As expected, incubation under capacitation conditions caused a dispersal in flotillin signal similar to the one caused by MβCD known to remove cholesterol from non-capacitated sperm (Fig. 6B). In order to study the kinetics and place of this process within the female environment, *post coitus* assays were performed. At time 0 *post coitus*, the endogenous SPINK3 signal was observed in the apical and flagellar regions of sperm obtained from the uterus (Fig. 7A), while 1.5 h later, only the flagellar signal was observed in sperm from the uterus and oviduct (Fig. 7B). After 3 h, sperm were observed interacting with the oviductal epithelium; however, there was no signal of SPINK3 (Fig. 7B). So, we can suggest that there is endogenous SPINK3 removal kinetics, where the apical mark would be the first to detach from the sperm and the flagellar bound protein would be lost later. These results are in line with the idea that DFs such as SPINK3 must be removed before reaching the oviduct for capacitation to take place.

Considering the physiological relevance of SPINK3 removal, we investigated the acrosomal status of the sperm cells simultaneously with SPINK3 presence. According to what we expected, the percentage of reacted sperm in the uterus and the oviduct was higher at 3 h *post coitus* compared to 1.5 h (data not shown). We observed that no SPINK3 signal was present over the sperm surface in the acrosome reacted cells, while immunolabeling was found in non-reacted sperm (Fig. 8), supporting that removal should take place before AR or that only sperm that lost the DF were able to react. Removal mechanisms of DFs are still unrevealed. Anchor receptors and mesmbrane destabilization are some of the hypothesized explanations. Based on the evidence that detachment starts in the uterus, we wondered whether UF from estrus females could remove recombinant SPINK3 from non-capacitated sperm. To test this, we pre-incubated sperm with SPINK3, then exposed them with UF from females in estrus (EUF) or metaestrus (MUF) for 15 or 30 min and evaluated SPINK3 presence in these cells. The SPINK3 label from the apical zone and the flagellum was reduced in cells incubated with EUF but not EUM at both times (Fig. 9). These results suggest that the environment of UF from estrus females

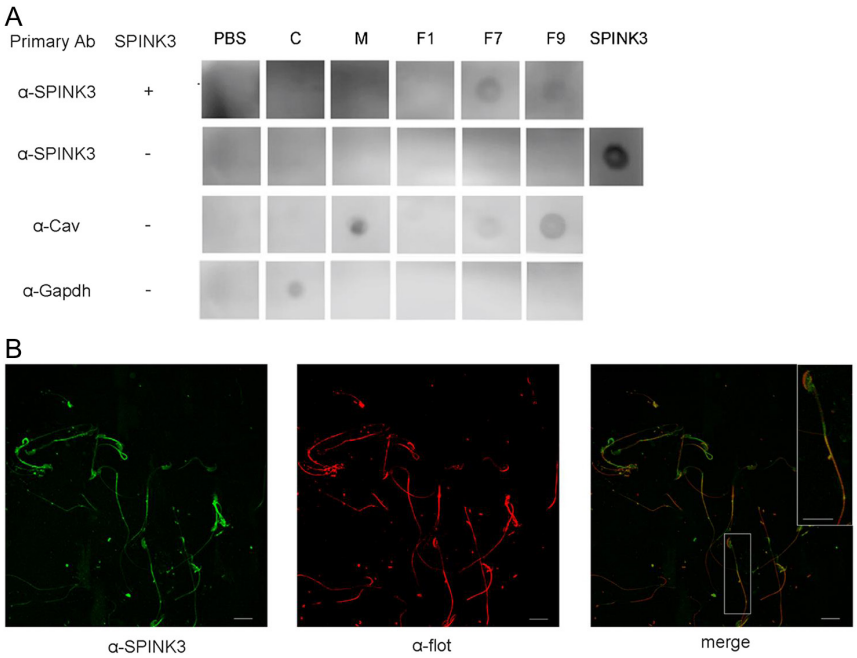

Figure 4 SPINK3-His_6 binds specific sperm cellular fractions. (A) Sperm subcellular fractions were spot seeded on a nitrocellulose membrane and incubated with (+) and without (–) SPINK3-His_6 (13 μM). C) or M fractions were spotted. Fractions 1–9 were collected from the top to the bottom of the isopycnic gradient being fraction 7 the one that contains the pure raft domains. Binding of SPINK3-His_6 to each fraction was developed with α-SPINK3 antibody. As a positive control, pure recombinant SPINK-His_6 was dotted (3 μg) (on the right last column: SPINK3). Subcellular fractions were immunologically identified by their specific markers: caveolin (α-Cav, raft marker), or glyceraldehyde phosphate dehydrogenase (α-Gapdh, cytosolic marker). (B) Immunolocalization of SPINK3-His_6 and flotillin on the sperm surface. Mouse epididymis cauda sperm were incubated in the presence of SPINK3-His_6 (13 μM) and immunofluorescence assays were developed by mouse anti-SPINK3 (α-SPINK3) and rabbit anti-flotillin (α-flot) followed by anti-mouse IgG-Alexa488 (green) and anti-rabbit IgG-Alexa555 (red). MERGE: red and green channels. Scale bar: 10 μm. The images are representative images from three independent experiments. C, cystolic; M, membrane.

could remove the recombinant protein SPINK3 from the sperm surface.

In order to evaluate if there is any protein–protein interaction that might be responsible for detaching the SPINK3, UF from estrus females was confronted to immobilized SPINK3 in an assay similar to the one described in Fig. 2. In this case, a number of proteins were retained by the column (Fig. 10). However, the proteomic analysis did not find secreted proteins candidates to interact with SPINK3 (data not shown). These results further substantiates that SPINK3, a protein that prevents acquisition of fertilizing competence, is removed from sperm by *in vitro* and *in vivo* capacitating environments without the participation of an exogenous protein.

Discussion

Sperm capacitation agonists have been widely studied in mammals; however, little is known regarding the mechanisms that avoid premature capacitation. Decapacitation proteins from seminal plasma play a fundamental role for the sperm to acquire their fertilizing capacity at the correct time and place. In the mouse, several potential DFs were characterized in seminal plasma, including seminal vesicle autoantigen (Huang *et al.* 2000), phosphatidylethanolamine binding protein 1 (PBP) (Nixon *et al.* 2006), seminal vesicle secretion 2 (Kawano *et al.* 2008), SPINKL (Lin *et al.* 2008), serpin peptidase inhibitor, clade E, member 2 (Lu *et al.* 2011) and SPINK3 (Assis *et al.* 2013) which are secreted by the seminal vesicles, and the epididymis-secreted a 40-kDa glycoprotein (Fraser *et al.* 1990). In other species, DFs have also been identified in seminal plasma, such as semenogelin in humans (de Lamirande *et al.* 2001), Kazal type 2/acrosin inhibitor in boar (Zigo *et al.* 2019) and the secretory protein rich in cysteine secreted by the epididymis 1 identified in rats (Roberts *et al.* 2003). SPINK3, is a Kazal type 3 serine protease inhibitor (Zalazar *et al.* 2012). Once this protein is secreted by the seminal vesicle it has the ability to bind to the sperm surface (Chen *et al.* 1998, Zalazar *et al.* 2012). Mature SPINK3 adheres both to the sperm head (Zalazar *et al.* 2012) and principal piece (Zalazar *et al.* 2020), inhibits intracellular calcium increase during capacitation and membrane hyperpolarization (Dematteis *et al.* 2008, Zalazar *et al.* 2012, 2020) impairing the sperm acrosome reaction and zona binding (Boettger-Tong *et al.* 1993), regardless of its trypsin inhibitory activity (Ou *et al.* 2012, Zalazar *et al.* 2012). Capacitation is negatively regulated by this protein, until it apparently detaches in the uterus (Ou *et al.* 2012).

In this work, we use two approaches to study SPINK3 binding and detachment from mouse sperm from the epididymis to the female duct. We performed *in vitro* assays with recombinant SPINK3 and *ex vivo post coitus* assays. The concentration of recombinant SPINK3 was chosen to resemble physiological doses in seminal vesicle secretions (~ 0.1 mg/mL- Coronel *et al.* 1992, Dematteis *et al.* 2008, Ou *et al.* 2012, Zalazar *et al.* 2012). We show that SPINK3 selectively attaches to mature mouse sperm and that this binding occurs to raft

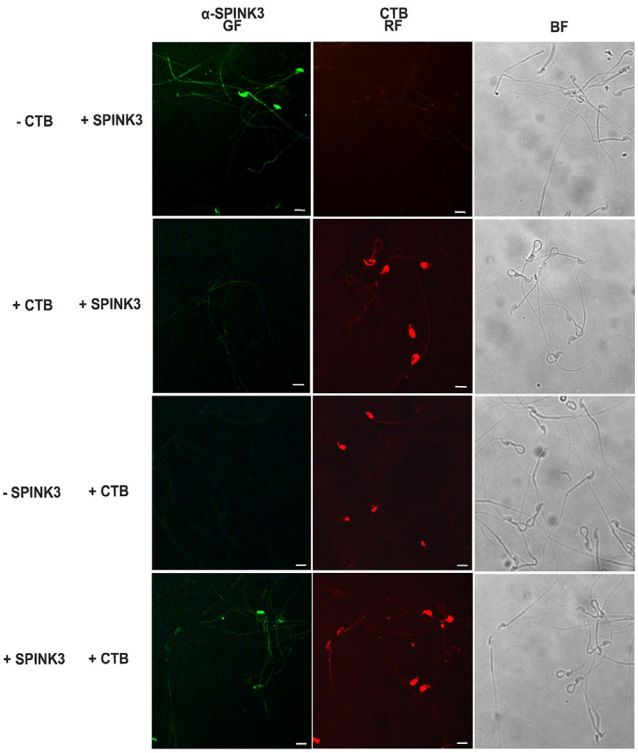

Figure 5 Competition assay between CTB and SPINK3 for GM1-rich regions. Mouse epididymis cauda sperm were incubated in the presence (+) or absence (–) of CTB (4 mM) and SPINK3-His_6 (13 μM). The order of addition of either CTB and SPINK3 is indicated at the left. SPINK3 was detected by immunofluorescence using anti-SPINK3 (α-SPINK3) followed by anti-rabbit IgG-Alexa488 (green), while CTB-Alexa594 was detected as red fluorescence. Scale bar: 10 μm. The images are representative images from three independent experiments. BF, bright field; GF, green field; RF, red field.

domains of the membrane. No protein ligand was found but instead, there was affinity *in vitro* between SPINK3 and PS and PC lipids. Additionally, we show that SPINK3 detachment from the sperm head starts in the female uterus at the head and later in the oviduct at the tail and that no sperm has bound protein in the oviduct at 3 h *post coitus*. This detachment occurs under *in vivo* and *in vitro* capacitation conditions which are sufficient to promote SPINK3 release, as no external SPINK3–protein interaction is found.

SPINK3–sperm binding has been demonstrated in different mammalian species such as the mouse (Irwin *et al.* 1983, Chen *et al.* 1998), human (Dietl *et al.* 1976), wild boar (Schill *et al.* 1975) and bull (Veselský & Čechová 1980); however, to date, its binding mechanism to sperm cells is still unrevealed. It is known that during sperm maturation, protein-protein type associations are generated on its surface (Aarons *et al.* 1985), in which glycoproteins, proteins with fibronectin domains, serine proteases, and inhibitors are found (Monclus *et al.* 2007). Following this line, we studied whether there was a protein-protein interaction holding SPINK3 to the sperm surface. We were unable to retain and identify, under the conditions studied, a sperm protein bound to SPINK3 bait. Curiously, a recent publication simultaneous to this work found the serine protease TESP1 as the protein receptor for SPINK3 at the sperm head by using a photoaffinity labeling assay (Ramachandran *et al.* 2021). To date, no ligand for SPINK3 was found on the sperm principal piece. Our failure to find this interactor can be explained in the partial homology between serine protease peptides and trypsin from *Sus scrofa* used for peptide digestion as these peptides were filtered from our peptide matching. Previous works have shown that other secretory proteins and DFs have the ability to interact with the outer layer of the plasma membrane through protein–lipid interactions (Glomset 1999, Manjunath & Thérien 2002, Brewis & Gadella 2009). Mouse PBP is a phosphatidylethanolamine binding protein found on mouse sperm, while the binder of sperm proteins family contains repeated fibronectin type 2 domains that are known to bind choline phospholipids (Kutty *et al.* 2014). Spermadhesins interact with sperm phospholipids and exhibit carbohydrate-binding activity with molecules from the female tract (Töpfer-Petersen *et al.* 1998, Schröter 2017). In human sperm, glycodelin-S has been proposed to bind membrane cholesterol serving as an anchoring mechanism and decapacitation action by preventing cholesterol removal (Chiu *et al.* 2005). Some sperm-bound proteins, mostly secreted by the epididymis, were found on the monosialotetrahexosylganglioside GM1 rich fraction of the sperm membrane (Asano *et al.* 2009, 2010). We found that SPINK3 is able to bind to the plasma membrane specifically in the regions where lipids rafts are found, and to pure PS and PC. PS is mostly localized typically in the inner cytoplasmic leaflet with the exception of several physiological conditions. However, there are studies showing that externalized PS is localized at the lipid raft regions in viable activated immune cells (Ishii *et al.* 2005), and on the sperm head region of viable and motile sperm, progressively increasing during sperm transit through the epididymis (i.e. non-capacitated sperm), (Rival *et al.* 2019). Besides we were able to demonstrate that there is a basal exposure of PS in non-capacitated sperm, this has been found over the post acrosomal and midpiece regions, different from the pattern of SPINK3 binding (Fig. 3C). In our work, SPINK3 is bound to flotillin and GM1 rich regions, and CTB avoids this binding, suggesting that anchoring of this DF is to raft membrane microdomains. Further work is needed to understand if binding to the head and the tail are mediated by the same target molecules.

For the sperm to acquire their fertilizing capacity, SPINK3, is one of the decapacitation proteins that must be removed in the female tract. A dramatic remodeling of the membrane is a hallmark of capacitation, with the redistribution and loss of certain components such as lipids and proteins. It is assumed that normal sperm

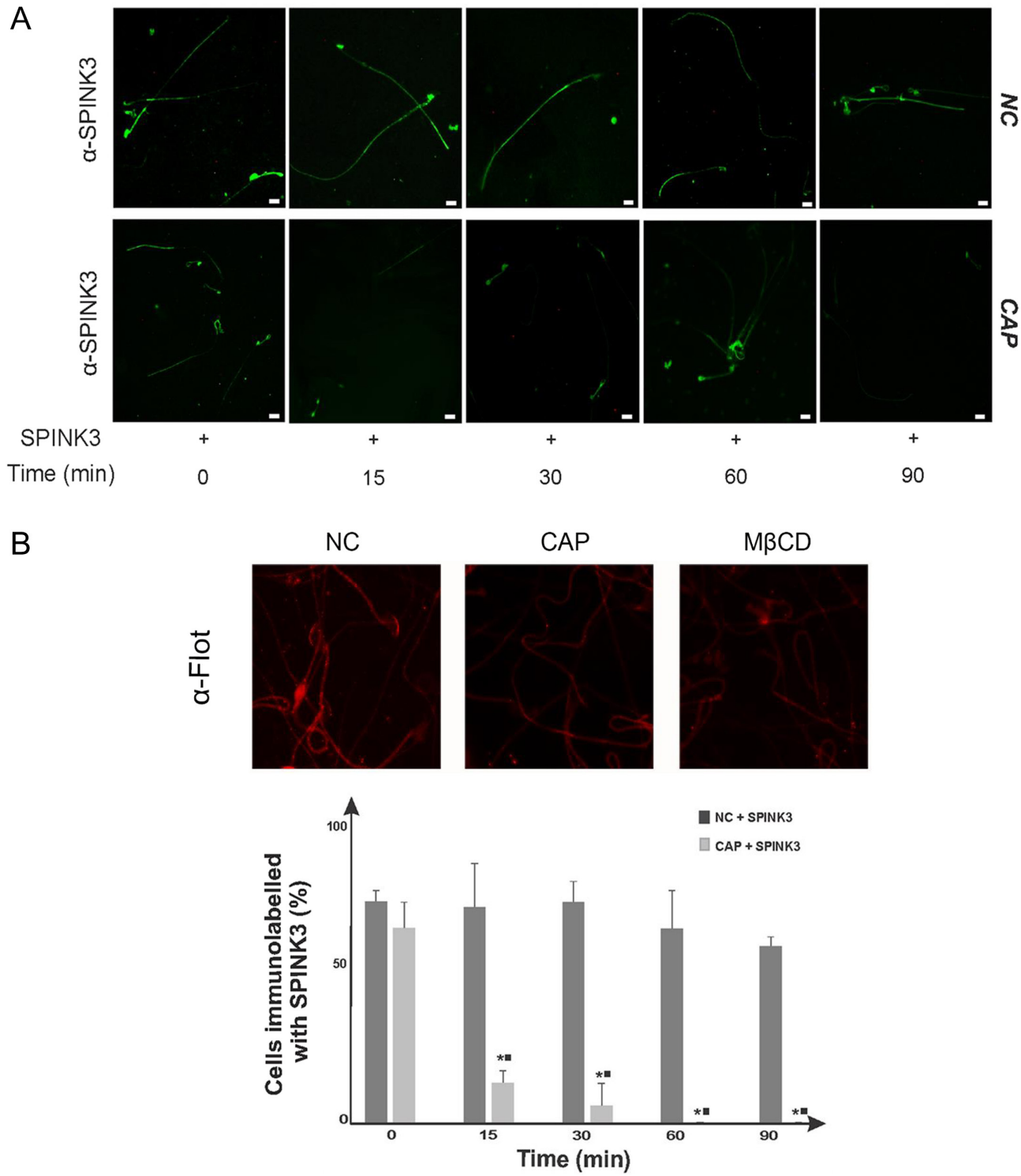

Figure 6 Removal of SPINK3-His_6 from the sperm surface by *in vitro* capacitation. (A) Mouse cauda sperm were incubated for 15 min with SPINK3-His_6 (13 µM). Then they were incubated under capacitating (CAP) or non-capacitating media (NC control) for different times. The presence of SPINK3-His_6 on the sperm surface was evaluated by immunofluorescence. Top panel shows representative pseudocolor (α-SPINK3, green) images. Scale bar: 10 µm. Bottom panel shows the percentage of positive immunoreactive cells (fluorescence in the apical region and/or in the main piece) after the different treatments, as indicated. *Significant differences with respect to its corresponding control (not capacitated with SPINK3-His_6). (■) Significant differences with respect to time 0. (B) Raft destabilization during capacitation evidenced by flotillin fading. Immunofluorescence assays were developed by rabbit anti-flotillin (α-flot) as described in Fig. 4B. Representative images are shown from three independent replicates. CAP, capacitated sperm; MβCD, cholesterol efflux triggered by methyl-β-cyclodextrin; NC, non-capacitated sperm.

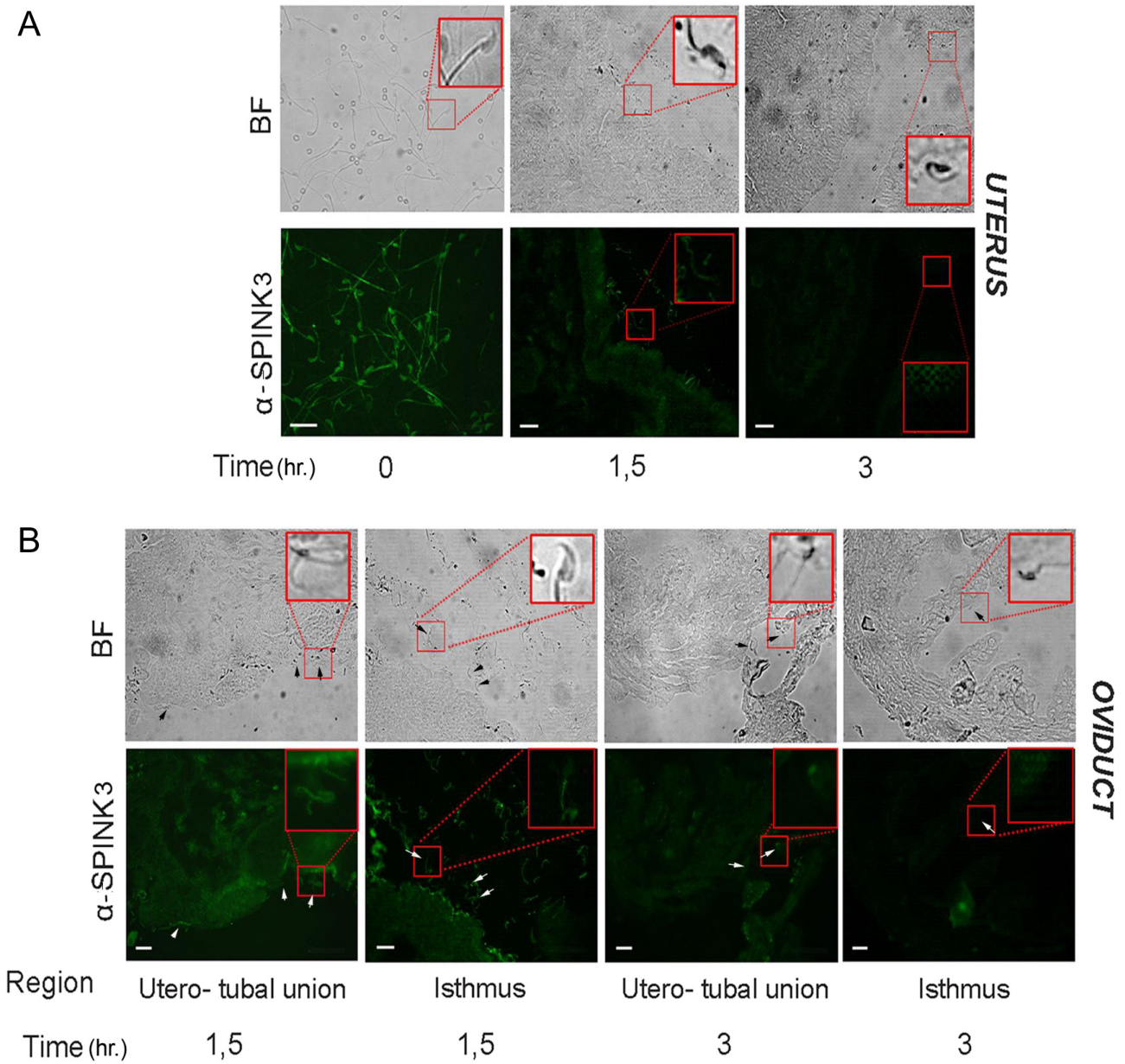

Figure 7 SPINK3 removal kinetics in the female tract. Estrus females were placed with sexually mature males and the presence of a vaginal plug was determined. Euthanasia was performed at 0, 1.5 and 3 h *post coitus* and the uterus–oviduct region was dissected. The presence of endogenous SPINK3 was evaluated by immunofluorescence with anti-SPINK3 (α-SPINK3). (A) Sperm bound SPINK3 in the uterus at 0, 1.5 and 3 h *post coitus*. (B) Sperm bound SPINK3 in different regions of the oviduct at 1.5 and 3 h *post coitus*. Arrows (→) indicate the presence of spermatozoa. The images are representative of three independent experiments. Scale bar: 20 μm. BF, bright field.

capacitation takes place in the oviduct after being released from the oviductal epithelium. Accordingly, previous studies had already shown that SPINK3 bound to the apical head hook was present at the uterus but absent in the sperm recovered from the oviduct lumen (Ou *et al.* 2012); however, no kinetics were reported and there is no mention of the protein bound to the principal piece. When we evaluated the removal of endogenous SPINK3, we observed that the signal in the apical region is removed prior to that of the flagellar region and that this removal occurs within the uterus, which suggests an orderly process. This might be mediated by uterine molecules or either by the environmental conditions that pursue sperm membrane remodeling and/or sperm physiology changes. We can also hypothesize that different mechanisms mediate detachment of SPINK3 from the head and from the tail, as the time and place of the processes are distinct. As our approach is based on antibody labeling, it cannot be ruled out a SPINK3 coating within the female environment, being

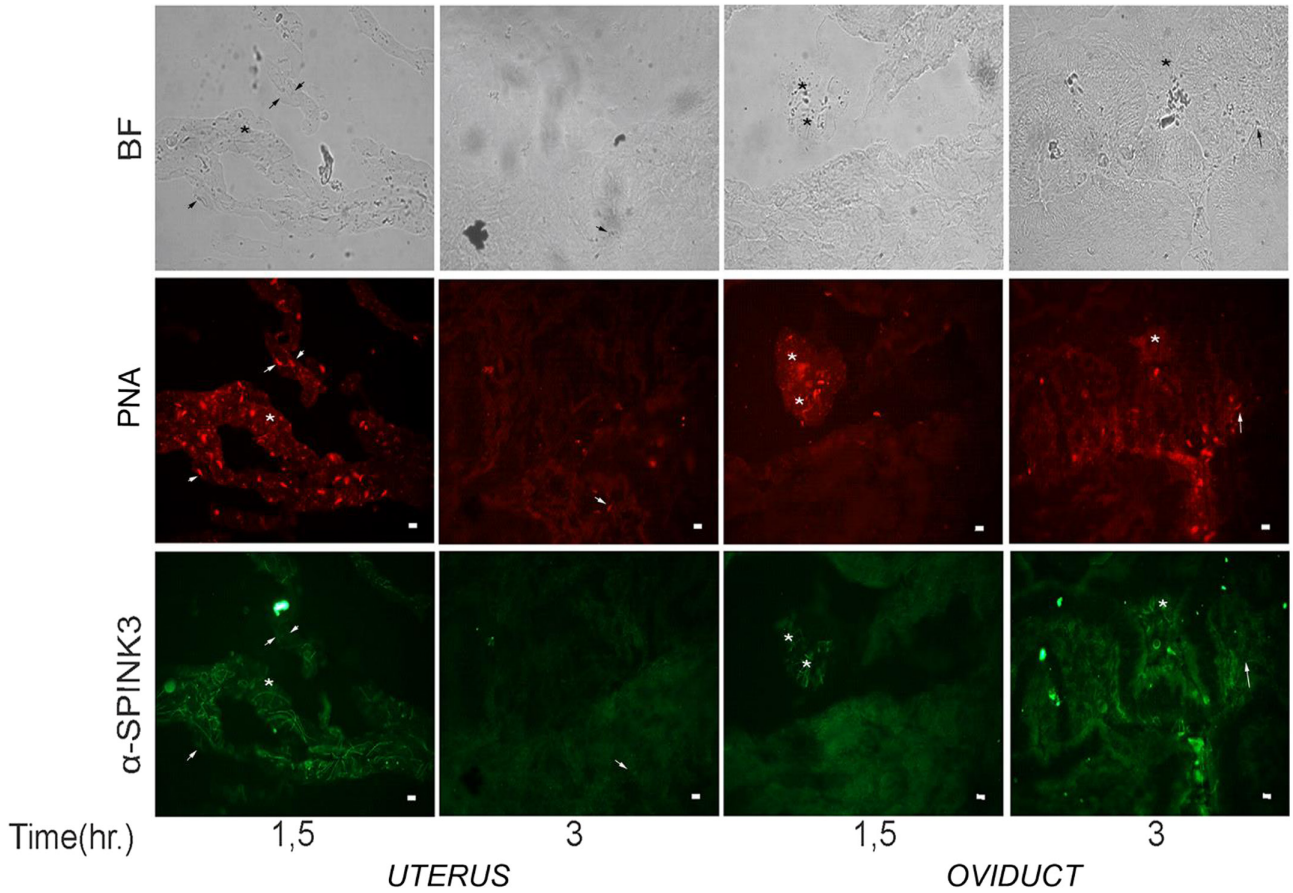

Figure 8 SPINK3 detachment precedes acrosomal reaction in the female tract. *Ex vivo* cryosections were performed for immunodetection of endogenous SPINK3 in spermatozoa in the uterus or oviduct at 1.5 or 3 h *post coitus*. The extent of the acrosome reaction was judged by PNA-Alexa 594 labeling (PNA, red). Endogenous SPINK3 labeling was assessed by immunofluorescence with anti-SPINK3 antibodies followed by anti-rabbit IgG-Alexa488 conjugated (α-SPINK3, green). Arrows (→) indicate the presence of acrosome reacted spermatozoa without SPINK3 labeling. Asterisks (*) indicate the presence of intact SPINK3-labeled sperm. The images are representative of three independent experiments. Scale bar: 10 µm. BF, brightfield.

inaccessible to its specific antibodies. Delayed removal from the tail is in agreement with our previous report demonstrating that the effective decapacitating action of SPINK3 is due to some inhibitory activity over CatSper channel and/or Slo3 channel (Zalazar *et al.* 2020), both localized at sperm principal piece (Navarro *et al.* 2007, Chung *et al.* 2014, Hwang *et al.* 2019). The activation kinetics of these channels (Ritagliati *et al.* 2018) in consonance with the proposal that changes associated with capacitation go from the tail to the head, which would accompany the order in which SPINK3 detaches itself from the spermatozoa. Further investigation is necessary to understand the role of each SPINK3 binding region and to determine if the receptor molecule is the same at both zones. Our work suggests that SPINK3 early detachment might permit sperm subpopulations to undergo acrosomal exocytosis in the uterus and after that time most sperm cells reacted in the oviduct. Regarding the AR, we confirmed that SPINK3 is no longer present on the surface of sperm that already underwent AR, which is in line with the kinetics of the capacitation, that is prior to the AR. La Spina and co-workers (La Spina *et al.* 2016) showed that a significant number of sperm that reaches the upper isthmus had already undergone acrosomal exocytosis, and in this work, we also found AR sperm in the uterus. Additional research in the mouse system is required to understand whether the early capacitated sperm or the late population that conserve DFs lately are the ones that would be successful to fertilize the ovum.

About the molecular mechanism that enhances the removal of SPINK3 in the female tract, we hypothesize that the capacitating female environment should be responsible for this detachment. In this sense, raft destabilization promoted by capacitating conditions might contribute to SPINK3 detachment. Our results carried out *in vitro* demonstrated that the interaction of sperm pre-incubated with recombinant SPINK3 with fluid from estrus females and with capacitating media removes the decapacitation protein from the surface of both the head and the tail after 15 min, with no further

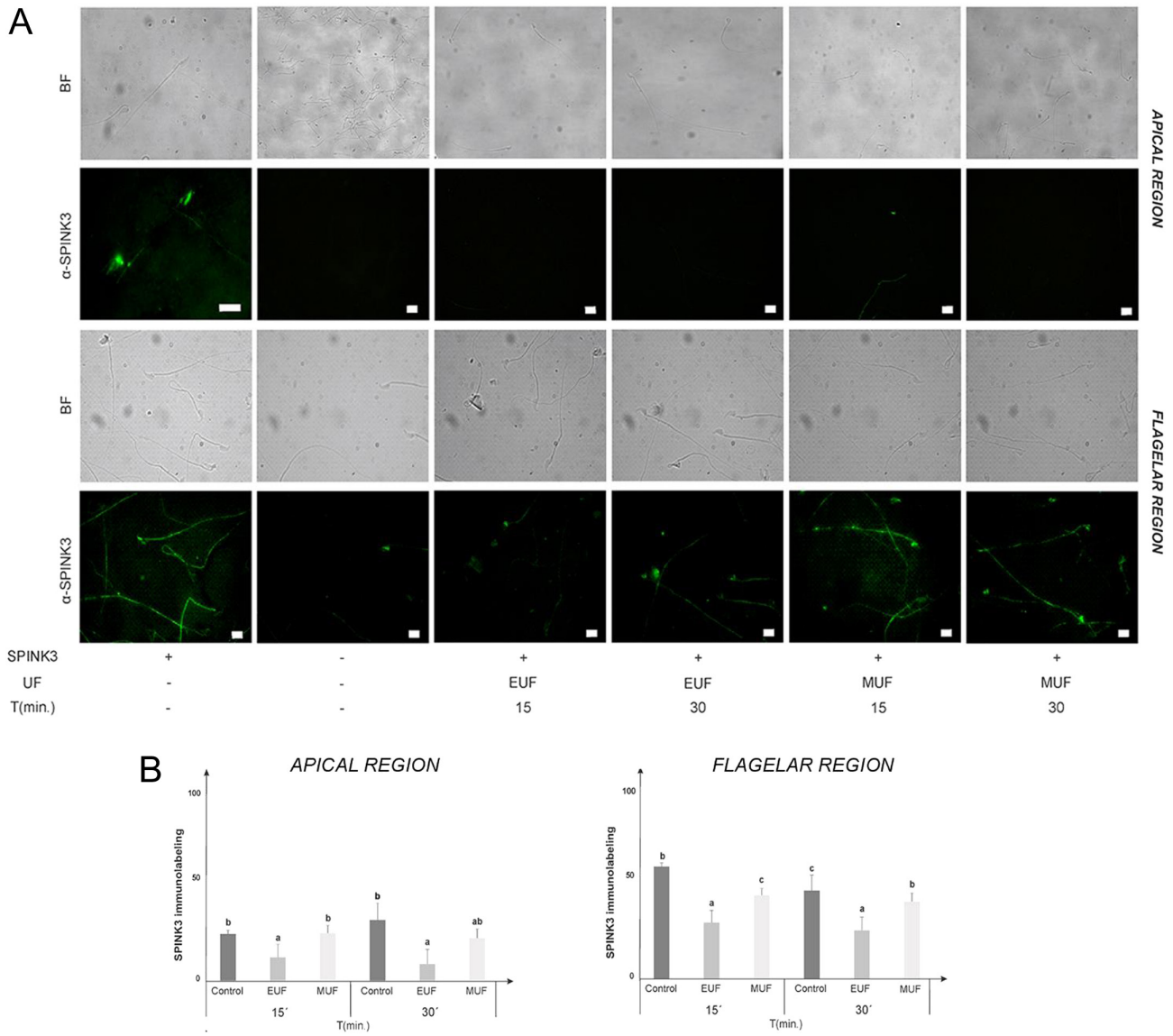

Figure 9 *In vitro* SPINK3-His$_6$ detachment by UF from estrus or metaestrus females. (A) Mouse cauda sperm were incubated for 15 min with or without SPINK3-His$_6$ (13 μM). Then they were confronted with EUF, MUF or non-capacitating buffer (control UF−) for 15 or 30 min. The presence of SPINK3-His$_6$ on the sperm surface was evaluated by immunofluorescence. Left panel shows representative pseudocolor (α-SPINK3, green) images and their corresponding BF. Scale bar: 10 μm. Representative images from three independent replicates. (B) Percentage of positive immunoreactive cells in the apical region or in the main piece after the different treatments, as indicated. Different letters indicate significant differences ($P \leq 0.05$) within the time of incubation between treatments. BF, bright field; EUF, UF from females in estrus; MUF, UF from females in metaestrus; UF, uterine fluid.

change after 30 min. This *in vitro* remotion did not mimic the head-tail kinetic observed *in vivo*. The ability to remove SPINK3 of the estrus fluid was significantly higher than those from metaestrus, suggesting that there would be signals, associated to the reproductive competence, mediating this removal. However, our protein-protein interaction assay did not trap any protease or other significant secretory protein from the UF. Otherwise, sperm–epithelia interaction necessary for capacitation (Gimeno *et al.* 2021) might support the idea that orderly and localized DF removal might take place only during this interaction.

In conclusion, this work presents for the first time molecular, kinetics and environmental insights into the way in which a decapacitation protein, SPINK3, is attached and later removed from the mouse sperm surface explaining in part how they regulate capacitation time and place.

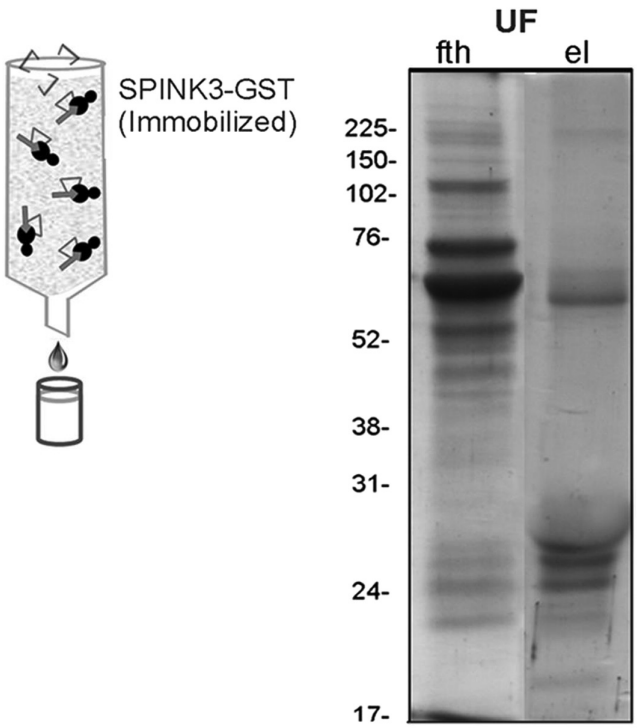

Figure 10 Protein–protein interactions between SPINK3 and proteins from the UF. UF was confronted to immobilized GST-SPINK3 or GST in an assay similar to the one described in Fig. 2. Electrophoretic separation of protein interactors from UF. Flowthrough (fth) and eluted (el) proteins (5 µg) obtained from GST-SPINK3-linked column, were separated by SDS-PAGE in 12% polyacrylamide gels. UF, uterine fluid.

Declaration of interest

The authors declare that there is no conflict of interest that could be perceived as prejudicing the impartiality of the research reported.

Funding

This work was supported by grants from the National Scientific and Technical Research Council (CONICET, Argentina, PIP 11220130100273) and from ANPCyT (PICT 2015-3682) both awarded to A C.

Data availability statement

All datasets generated for this study are included in the article.

Author contribution statement

A C and S P M contributed to the conceptualization of the study, supervision, and project administration. A N, C O and C A I A contributed to the design and development of the methodology. A P, M C and V S contributed to perform the proteomic analysis. A N, A C and L Z contributed to the writing and editing of the manuscript. All the co-authors were involved in the formal analysis, validation, visualization of the results and revised the manuscript.

Acknowledgements

The authors would like to thank Marcelo C F Guagnini for the cryocuts and Viviana Daniel and Daniela Villamonte for their assistance during confocal microscopy. The authors also acknowledge Hugo Nuñez for his assistance with the animal handling and maintenance.

References

Aarons D, Robinson R, Richardson R & Poirier GR 1985 Competition between seminal and exogenous proteinase inhibitors for sites on murine epididymal sperm. *Contraception* **31** 177–184. (https://doi.org/10.1016/0010-7824(85)90032-0)

Asano A, Selvaraj V, Buttke DE, Nelson JL, Green KM, Evans JE & Travis AJ 2009 Biochemical characterization of membrane fractions in murine sperm: identification of three distinct sub-types of membrane rafts. *Journal of Cellular Physiology* **218** 537–548. (https://doi.org/10.1002/jcp.21623)

Asano A, Nelson JL, Zhang S & Travis AJ 2010 Characterization of the proteomes associating with three distinct membrane raft sub-types in murine sperm. *Proteomics* **10** 3494–3505. (https://doi.org/10.1002/pmic.201000002)

Assis DM, Zalazar L, Aparecida Juliano MA, De Castro R & Cesari A 2013 Novel inhibitory activity for serine protease inhibitor Kazal type-3 (Spink3) on human recombinant kallikreins. *Protein and Peptide Letters* **20** 1098–1107. (https://doi.org/10.2174/0929866511320100003)

Austin CR 1952 The 'capacitation' of the mammalian sperm. *Nature* **170** 326–326. (https://doi.org/10.1038/170326a0)

Bedford JM & Chang MC 1962 Removal of decapacitation factor from seminal plasma by high-speed centrifugation. *American Journal of Physiology* **202** 179–181. (https://doi.org/10.1152/ajplegacy.1962.202.1.179)

Bligh EG & Dyer WJ 1959 A rapid method of total lipid extraction and purification. *Canadian Journal of Biochemistry and Physiology* **37** 911–917. (https://doi.org/10.1139/o59-099)

Boettger-Tong HL, Aarons DJ, Biegler BE, George B & Poirier GR 1993 Binding of a murine proteinase inhibitor to the acrosome region of the human sperm head. *Molecular Reproduction and Development* **36** 346–353. (https://doi.org/10.1002/mrd.1080360310)

Brewis IA & Gadella BM 2009 Sperm surface proteomics: from protein lists to biological function. *MHR: Basic Science of Reproductive Medicine* **16** 68–79. (https://doi.org/10.1093/molehr/gap077)

Byers SL, Wiles MV, Dunn SL & Taft RA 2012 Mouse estrous cycle identification tool and images. *PLoS ONE* **7** e35538. (https://doi.org/10.1371/journal.pone.0035538)

Cerletti M, Paggi R, Troetschel C, Ferrari MC, Guevara CR, Albaum S, Poetsch A & De Castro R 2018*a* LonB protease is a novel regulator of carotenogenesis controlling degradation of phytoene synthase in Haloferax volcanii. *Journal of Proteome Research* **17** 1158–1171. (https://doi.org/10.1021/acs.jproteome.7b00809)

Cerletti M, Giménez MI, Tröetschel C, D'Alessandro C, Poetsch A, De Castro RE & Paggi RA 2018*b* Proteomic study of the exponential–stationary growth phase transition in the haloarchaea Natrialba magadii and Haloferax volcanii. *Proteomics* **18** e1800116. (https://doi.org/10.1002/pmic.201800116) 29888524.

Cesari A, de los Angeles Monclus Mde L, Tejón GP, Clementi M & Fornes MW 2010 Regulated serine proteinase lytic system on mammalian sperm surface: there must be a role. *Theriogenology* **74** 699.e1–711.e1. (https://doi.org/10.1016/j.theriogenology.2010.03.029)

Chang MC 1951 Fertilizing capacity of spermatozoa deposited into the fallopian tubes. *Nature* **168** 697–698. (https://doi.org/10.1038/168697b0)

Chang MC 1957 A detrimental effect of seminal plasma on the fertilizing capacity of sperm. *Nature* **179** 258–259. (https://doi.org/10.1038/179258a0)

Chen LY, Lin YH, Lai ML & Chen YH 1998 Developmental profile of a caltrin-like protease inhibitor, P12, in mouse seminal vesicle and characterization

Q12

of its binding sites on sperm surface. *Biology of Reproduction* **59** 1498–1505. (https://doi.org/10.1095/biolreprod59.6.1498)

Chiu PC, Chung MK, Tsang HY, Koistinen R, Koistinen H, Seppala M, Lee KF & Yeung WS 2005 Glycodelin-S in human seminal plasma reduces cholesterol efflux andInhibits capacitation ofSpermatozoa. *Journal of Biological Chemistry* **280** 25580–25589. (https://doi.org/10.1074/jbc.M504103200)

Chung JJ, Shim SH, Everley RA, Gygi SP, Zhuang X & Clapham DE 2014 Structurally distinct Ca2+ signaling domains of sperm flagella orchestrate tyrosine phosphorylation and motility. *Cell* **157** 808–822. (https://doi.org/10.1016/j.cell.2014.02.056)

Coronel CE, Winnica DE, Novella ML & Lardy HA 1992 Purification, structure, and characterization of caltrin proteins from seminal vesicle of the rat and mouse. *Journal of Biological Chemistry* **267** 20909–20915. (https://doi.org/10.1016/S0021-9258(19)36774-2)

Cross NL 2004 Reorganization of lipid rafts during capacitation of human sperm. *Biology of Reproduction* **71** 1367–1373. (https://doi.org/10.1095/biolreprod.104.030502)

de Lamirande E, Yoshida K, Yoshiike TM, Iwamoto T & Gagnon C 2001 Semenogelin, the main protein of semen coagulum, inhibits human sperm capacitation by interfering with the superoxide anion generated during this process. *Journal of Andrology* **22** 672–679. (https://doi.org/10.1002/j.1939-4640.2001.tb02228.x)

Dematteis A, Miranda SD, Novella ML, Maldonado C, Ponce RH, Maldera JA, Cuasnicu PS & Coronel CE 2008 Rat caltrin protein modulates the acrosomal exocytosis during sperm capacitation. *Biology of Reproduction* **79** 493–500. (https://doi.org/10.1095/biolreprod.107.067538)

Dietl T, Kruck J, Schill WB & Fritz H 1976 Localization of seminal plasma proteinase inhibitors in human spermatozoa as revealed by the indirect immunofluorescence technique. *Hoppe-Seyler's Zeitschrift für Physiologische Chemie* **357** 1333–1337. (https://doi.org/10.1515/bchm2.1976.357.2.1333)

Fraser LR 1984 Mouse sperm capacitation in vitro involves loss of a surface-associated inhibitory component. *Journal of Reproduction and Fertility* **72** 373–384. (https://doi.org/10.1530/jrf.0.0720373)

Fraser LR, Harrison RAP & Herod JE 1990 Characterization of a decapacitation factor associated with epididymal mouse spermatozoa. *Journal of Reproduction and Fertility* **89** 135–148. (https://doi.org/10.1530/jrf.0.0890135)

Gimeno BF, Bariani MV, Laiz-Quiroga L, Martínez-León E, Von-Meyeren M, Rey O, Mutto AÁ & Osycka-Salut CE 2021 Effects of in vitro interactions of oviduct epithelial cells with frozen–thawed stallion spermatozoa on their motility, viability and capacitation status. *Animals* **11** 74. (https://doi.org/10.3390/ani11010074)

Glomset JA 1999 Lipids protein-lipid interactions on the surfaces of cell membranes. *Current Opinion in Structural Biology* **9** 425–427. (https://doi.org/10.1016/s0959-440x(99)80058-x)

Graf CB, Ritagliati C, Stival C, Luque GM, Gentile I, Buffone MG & Krapf D 2020 Everything you ever wanted to know about PKA regulation and its involvement in mammalian sperm capacitation. *Molecular and Cellular Endocrinology* **518** 110992. (https://doi.org/10.1016/j.mce.2020.110992)

Harrison RA & Gadella BM 2005 Bicarbonate-induced membrane processing in sperm capacitation. *Theriogenology* **63** 342–351. (https://doi.org/10.1016/j.theriogenology.2004.09.016)

Huang YH, Chu ST & Chen YH 2000 A seminal vesicle autoantigen of mouse is able to suppress sperm capacitation-related events stimulated by serum albumin. *Biology of Reproduction* **63** 1562–1566. (https://doi.org/10.1095/biolreprod63.5.1562)

Hummel KM, Penheiter AR, Gathman AC & Lilly WW 1996 Anomalous estimation of protease molecular weights using gelatin-containing SDS–PAGE. *Analytical Biochemistry* **233** 140–142. (https://doi.org/10.1006/abio.1996.0019)

Hwang JY, Mannowetz N, Zhang Y, Everley RA, Gygi SP, Bewersdorf J, Lishko PV & Chung JJ 2019 Dual sensing of physiologic pH and calcium by EFCAB9 regulates sperm motility. *Cell* **177** 1480.e19–1494.e19. (https://doi.org/10.1016/j.cell.2019.03.047)

Irwin M, Nicholson N, Haywood JT & Poirier GR 1983 Immunofluorescent localization of a murine seminal vesicle proteinase inhibitor. *Biology of Reproduction* **28** 1201–1206. (https://doi.org/10.1095/biolreprod28.5.1201)

Ishii H, Mori T, Shiratsuchi A, Nakai Y, Shimada Y, Ohno-Iwashita Y & Nakanishi Y 2005 Distinct localization of lipid rafts and externalized phosphatidylserine at the surface of apoptotic cells. *Biochemical and Biophysical Research Communications* **327** 94–99. (https://doi.org/10.1016/j.bbrc.2004.11.135)

Jalkanen J, Kotimäki M, Huhtaniemi I & Poutanen M 2006 Novel epididymal protease inhibitors with Kazal or WAP family domain. *Biochemical and Biophysical Research Communications* **349** 245–254. (https://doi.org/10.1016/j.bbrc.2006.08.023)

Kawano N, Yoshida K, Iwamoto T & Yoshida M 2008 Ganglioside GM1 mediates decapacitation effects of SVS2 on murine spermatozoa. *Biology of Reproduction* **79** 1153–1159. (https://doi.org/10.1095/biolreprod.108.069054)

Kazal LA, Spicer DS & Brahinsky RA 1948 Isolation of a crystalline trypsin inhibitor-anticoagulant protein from Pancreas1a. *Journal of the American Chemical Society* **70** 3034–3040. (https://doi.org/10.1021/ja01189a060)

Kherraf ZE, Christou-Kent M, Karaouzene T, Amiri-Yekta A, Martinez G, Vargas AS, Lambert E, Borel C, Dorphin B, Aknin-Seifer I *et al.* 2017 SPINK 2 deficiency causes infertility by inducing sperm defects in heterozygotes and azoospermia in homozygotes. *EMBO Molecular Medicine* **9** 1132–1149. (https://doi.org/10.15252/emmm.201607461)

Kutty MVH, Remya V, Shyma VH, Radhika S, Shende AM & Bhure SK 2014 An overview on binder of sperm proteins of cattle. *International Journal of Livestock Research* **4** 1–11. (https://doi.org/10.5455/ijlr.20140629034437)

La Spina FA, Molina LCP, Romarowski A, Vitale AM, Falzone TL, Krapf D, Hirohashi N & Buffone MG 2016 Mouse sperm begin to undergo acrosomal exocytosis in the upper isthmus of the oviduct. *Developmental Biology* **411** 172–182. (https://doi.org/10.1016/j.ydbio.2016.02.006)

Laemmli UK, Beguin F & Gujer-Kellenberger G 1970 A factor preventing the major head protein of bacteriophage T4 from random aggregation. *Journal of Molecular Biology* **47** 69–85. (https://doi.org/10.1016/0022-2836(70)90402-X)

Leahy T & Gadella BM 2011 Sperm surface changes and physiological consequences induced by sperm handling and storage. *Reproduction* **142** 759–778. (https://doi.org/10.1530/REP-11-0310)

Lenth RV 2016 Least-squares means: the R package lsmeans. *Journal of Statistical Software* **69** 1–33. (https://doi.org/10.18637/jss.v069.i01)

Lin MH, Lee RKK, Hwu YM, Lu CH, Chu SL, Chen YJ, Chang WC & Li SH 2008 SPINKL, a Kazal-type serine protease inhibitor-like protein purified from mouse seminal vesicle fluid, is able to inhibit sperm capacitation. *Reproduction* **136** 559–571. (https://doi.org/10.1530/REP-07-0375)

Lu CH, Lee RKK, Hwu YM, Chu SL, Chen YJ, Chang WC, Lin SP & Li SH 2011 SERPINE2, a serine protease inhibitor extensively expressed in adult male mouse reproductive tissues, may serve as a murine sperm decapacitation factor. *Biology of Reproduction* **84** 514–525. (https://doi.org/10.1095/biolreprod.110.085100)

Manchenko GP 2002 *Handbook of Detection of Enzymes on Electrophoretic Gels*. CRC Press. (https://doi.org/10.1201/9781420040531)

Manjunath P & Thérien I 2002 Role of seminal plasma phospholipid-binding proteins in sperm membrane lipid modification that occurs during capacitation. *Journal of Reproductive Immunology* **53** 109–119. (https://doi.org/10.1016/S0165-0378(01)00098-5)

Monclus MA, Cesari A, Cabrillana ME, Borelli PV, Vincenti AE, Burgos MH & Fornés MW 2007 Mouse sperm rosette: assembling during epididymal transit, in vitro disassemble, and oligosaccharide participation in the linkage material. *Anatomical Record* **290** 814–824. (https://doi.org/10.1002/ar.20555)

Navarro B, Kirichok Y & Clapham DE 2007 KSper, a pH-sensitive K+ current that controls sperm membrane potential. *PNAS* **104** 7688–7692. (https://doi.org/10.1073/pnas.0702018104)

Nixon B, MacIntyre DA, Mitchell LA, Gibbs GM, O'Bryan M & Aitken RJ 2006 The identification of mouse sperm-surface-associated proteins and characterization of their ability to act as decapacitation factors. *Biology of Reproduction* **74** 275–287. (https://doi.org/10.1095/biolreprod.105.044644)

Noda T & Ikawa M 2019 Physiological function of seminal vesicle secretions on male fecundity. *Reproductive Medicine and Biology* **18** 241–246. (https://doi.org/10.1002/rmb2.12282)

Odet F, Verot A & Le Magueresse-Battistoni B 2006 The mouse testis is the source of various serine proteases and serine proteinase inhibitors (serpins): serine proteases and serpins identified in Leydig cells are under

gonadotropin regulation. *Endocrinology* **147** 4374–4383. (https://doi.org/10.1210/en.2006-0484)

O'Rand MG, Widgren EE, Hamil KG, Silva EJ & Richardson RT 2011 Epididymal protein targets: a brief history of the development of epididymal protease inhibitor as a contraceptive. *Journal of Andrology* **32** 698–704. (https://doi.org/10.2164/jandrol.110.012781)

Ou CM, Tang JB, Huang MS, Sudhakar Gandhi PS, Geetha S, Li SH & Chen YH 2012 The mode of reproductive-derived Spink (serine protease inhibitor Kazal-type) action in the modulation of mammalian sperm activity. *International Journal of Andrology* **35** 52–62. (https://doi.org/10.1111/j.1365-2605.2011.01159.x)

Pinheiro J, Bates D, DebRoy S, Sarkar D & R Core Team 2007 nlme: Linear and nonlinear mixed effects models. R package version 3.1-155, (https://CRAN.R-project.org/package=nlme)

Puga Molina LC, Luque GM, Balestrini PA, Marín-Briggiler CI, Romarowski A & Buffone MG 2018 Molecular basis of human sperm capacitation. *Frontiers in Cell and Developmental Biology* **6** 72. (https://doi.org/10.3389/fcell.2018.00072)

Ramachandran SS, Balu R, Vilwanathan R, Jeyaraman J & Paramasivam SG 2021 A mouse testis serine protease, TESP1, as the potential SPINK3 receptor protein on mouse sperm acrosome. *Molecular Human Reproduction* **27** gaab059. (https://doi.org/10.1093/molehr/gaab059)

Raterman D & Springer MS 2008 The molecular evolution of acrosin in placental mammals. *Molecular Reproduction and Development* **75** 1196–1207. (https://doi.org/10.1002/mrd.20868)

Ritagliati C, Graf CB, Stival C & Krapf D 2018 Regulation mechanisms and implications of sperm membrane hyperpolarization. *Mechanisms of Development* **154** 33–43. (https://doi.org/10.1016/j.mod.2018.04.004)

Rival CM, Xu W, Shankman LS, Morioka S, Arandjelovic S, Lee CS, Wheeler KM, Smith RP, Haney LB, Isakson BE *et al.* 2019 Phosphatidylserine on viable sperm and phagocytic machinery in oocytes regulate mammalian fertilization. *Nature Communications* **10** 4456. (https://doi.org/10.1038/s41467-019-12406-z)

Roberts KP, Wamstad JA, Ensrud KM & Hamilton DW 2003 Inhibition of capacitation-associated tyrosine phosphorylation signaling in rat sperm by epididymal protein Crisp-1. *Biology of Reproduction* **69** 572–581. (https://doi.org/10.1095/biolreprod.102.013771)

Samanta L, Parida R, Dias TR & Agarwal A 2018 The enigmatic seminal plasma: a proteomics insight from ejaculation to fertilization. *Reproductive Biology and Endocrinology* **16** 41. (https://doi.org/10.1186/s12958-018-0358-6)

Sanllorenti PM, Tardivo DB & Conde RD 1992 Dietary level of protein regulates glyceraldehyde-3-phosphate dehydrogenase content and synthesis rate in mouse liver cytosol. *Molecular and Cellular Biochemistry* **115** 117–128. (https://doi.org/10.1007/BF00230321)

Schill WB, Heimburger N, Schiessler H, Stolla R & Fritz H 1975 Reversible attachment and localization of the acid-stable seminal plasma acrosin-trypsin inhibitors on boar spermatozoa as revealed by the indirect immunofluorescent staining technique. *Hoppe-Seyler's Zeitschrift fur physiologische Chemie* **356** 1473–1476.

Schröter F, Müller K, Müller P, Krause E & Braun BC 2017 Recombinant expression of porcine spermadhesin AWN and its phospholipid interaction: indication for a novel lipid binding property. *Reproduction in Domestic Animals* **52** 585–595. (https://doi.org/10.1111/rda.12953)

Shang X, Shen C, Liu J, Tang L, Zhang H, Wang Y, Wu W, Chi J, Zhuang H, Fei J *et al.* 2018 Serine protease PRSS55 is crucial for male mouse fertility via affecting sperm migration and sperm–egg binding. *Cellular and Molecular Life Sciences* **75** 4371–4384. (https://doi.org/10.1007/s00018-018-2878-9)

Sipila P, Jalkanen J, Huhtaniemi IT & Poutanen M 2009 Novel epididymal proteins as targets for the development of post-testicular male contraception. *Reproduction* **137** 379–389. (https://doi.org/10.1530/REP-08-0132)

Stival C, La Spina FA, Graf CB, Arcelay E, Arranz SE, Ferreira JJ, Le Grand S, Dzikunu VA, Santi CM, Visconti PE *et al.* 2015 Src kinase is the connecting player between protein kinase A (PKA) activation and hyperpolarization through SLO3 potassium channel regulation in mouse sperm. *Journal of Biological Chemistry* **290** 18855–18864. (https://doi.org/10.1074/jbc.M115.640326)

Töpfer-Petersen E, Romero A, Varela PF, Ekhlasi-Hundrieser M, Dostalova Z, Sanz L & Calvete JJ 1998 Spermadhesins: a new protein family. Facts, hypotheses and perspectives. *Andrologia* **30** 217–224. (https://doi.org/10.1111/j.1439-0272.1998.tb01163.x)

Tseng HC, Lee RKK, Hwu YM, Lu CH, Lin MH & Li SH 2013 Mechanisms underlying the inhibition of murine sperm capacitation by the seminal protein, SPINKL. *Journal of Cellular Biochemistry* **114** 888–898. (https://doi.org/10.1002/jcb.24428)

Turpeinen U, Koivunen E & Stenman UH 1988 Reaction of a tumour-associated trypsin inhibitor with serine proteinases associated with coagulation and tumour invasion. *Biochemical Journal* **254** 911–914. (https://doi.org/10.1042/bj2540911)

Tyanova S, Temu T, Sinitcyn P, Carlson A, Hein MY, Geiger T, Mann M & Cox J 2016 The Perseus computational platform for comprehensive analysis of (prote) omics data. *Nature Methods* **13** 731–740. (https://doi.org/10.1038/nmeth.3901)

Veselský L & Čechová D 1980 Distribution of acrosin inhibitors in bull reproductive tissues and spermatozoa. *Hoppe-Seyler's Zeitschrift fur Physiologische Chemie* **361** 715–722. (https://doi.org/10.1515/bchm2.1980.361.1.715)

Yamashita M, Honda A, Ogura A, Kashiwabara SI, Fukami K & Baba T 2008 Reduced fertility of mouse epididymal sperm lacking Prss21/Tesp5 is rescued by sperm exposure to uterine microenvironment. *Genes to Cells* **13** 1001–1013. (https://doi.org/10.1111/j.1365-2443.2008.01222.x)

Yanagimachi R 1994 Fertility of mammalian spermatozoa: its development and relativity. *Zygote* **2** 371–372. (https://doi.org/10.1017/S0967199400002240)

Zalazar L, Saez Lancellotti TE, Clementi M, Lombardo C, Lamattina L, De Castro R, Fornes MW & Cesari A 2012 SPINK3 modulates mouse sperm physiology through the reduction of nitric oxide level independently of its trypsin inhibitory activity. *Reproduction* **143** 281–295. (https://doi.org/10.1530/REP-11-0107)

Zalazar L, Alonso CAI, De Castro RE & Cesari A 2014 An alternative easy method for antibody purification and analysis of protein–protein interaction using GST fusion proteins immobilized onto glutathione–agarose. *Analytical and Bioanalytical Chemistry* **406** 911–914. (https://doi.org/10.1007/s00216-013-7533-6)

Zalazar L, Stival C, Nicolli AR, De Blas GA, Krapf D & Cesari A 2020 Male decapacitation factor SPINK3 blocks membrane hyperpolarization and calcium entry in mouse sperm. *Frontiers in Cell and Developmental Biology* **8** 575126. (https://doi.org/10.3389/fcell.2020.575126)

Zhou Y, Zheng M, Shi Q, Zhang L, Zhen W, Chen W & Zhang Y 2008 An epididymis-specific secretory protein HongrES1 critically regulates sperm capacitation and male fertility. *PLoS ONE* **3** e4106. (https://doi.org/10.1371/journal.pone.0004106)

Zigo M, Manaskova-Postlerova P, Jonakova V, Kerns K & Sutovsky P 2019 Compartmentalization of the proteasome-interacting proteins during sperm capacitation. *Scientific Reports* **9** 12583. (https://doi.org/10.1038/s41598-019-49024-0)

Zuur AF, Ieno EN, Walker N, Saveliev AA & Smith GM 2009 *Mixed Effects Models and Extensions in Ecology with R*. New York: SpringerGoogle Scholar.

Received 7 May 2021
First decision 3 June 2021
Revised manuscript received 14 February 2022
Accepted 22 February 2022